REPORT NO. 78
MARCH, 1954.

THE COLLEGE OF AERONAUTICS

CRANFIELD

Stress Concentrations in Swept Wing Panels Using Photoelastic Models

-by-

G.M. COILEY, D.C.Ae.

SUMMARY

A theoretical solution for stress concentrations as might occur in a swept wing, has been derived by E.H. Mansfield. This thesis applies photoelastic techniques to models of wing panels with various angles of sweep, with the object of verifying these equations.

The results confirm that high values of peak shear stress may be expected for large wedge angles, although the stress for small angles is underestimated. The direct stresses in the free edge determined experimentally show that the theoretical solution is invalid for large wedge angles, and stresses are high but do not change their sense. For small angles the stress is of opposite sign, and much greater in magnitude.

This work was carried out by the author in the Department of Aircraft Design and submitted as a thesis for the Diploma of the College.

MEP

LIST OF CONTENTS

LIST OF ILLUSTRATIONS

LIST OF SYMBOLS

$\hat{\sigma}$ = Maximum average direct stress in boom

σ_E = Direct stress in the free edge

τ = Peak shear stress in the plate along the boom

F = Model fringe value for tension

n = Fringe order

θ = Parameter of the isoclinic parallel to the boom at the apex of the wedge.

---

1. Introduction

It is reasonable to assume that the data available for determining the stress concentrations in wing panels with no sweep, will give reliable results when applied to a swept panel, providing the sweep is small. Modern aircraft however employ large angles of sweep, and this assumption cannot be made, and as no data is available which gives a reliable estimation of the effects of sweep, work in this field is obviously essential. The only theoretical work published is by E.H. Mansfield Ref. 1, and it provides a guide as to the way the stresses may be influenced. Unfortunately the equation for peak shear stress is invalid for large values of wedge angles, where information is needed most badly. The object of this thesis is to test the equations for peak shear stress, and direct stress in the free edge, and obtain quantitative results for a wide range of sweepback.

The photoelastic technique used differs from normal practice in that a sudden change in thickness of the model occurs adjacent to the point at which measurements are made. It is considered, however, that because the results for no sweep compare quite favourably with the reliable data available for this condition, the results will not be seriously affected when dealing with swept panels.

The requirement in the theoretical solution that the flexural rigidity of the booms is zero is not fulfilled, although a method of loading which minimises its influence is suggested.

2. Models and Photoelastic Apparatus

Models were constructed from C.R.39 sheet material, bonded with Araldite 'D'. After several test specimens had been tested it was decided that hot curing to improve the glue strength was unnecessary. Six models were made with β varying from 0 to 60°. A seventh model with similar dimensions but with only one boom, was made for $\beta = 30^{\circ}$. These models are shown in figs. 1 and 2.

A standard photoelastic bench was used with a lens polariscope and a 3.0in. field. Load was measured by a strain gauge link in the loading system, and a sensitive galvanometer. Load was applied to the model by two beams, to produce equal loading on each boom.

The material fringe value was found to be 104.4 lb. per inch per fringe, in tension.

/ 3. ...

3. Description of Tests

The isoclinics were obtained by sketching on tracing paper placed over a ground glass screen. Only the centre of the field was used in order to minimise spherical aberration, and the load was varied to give maximum clearness. A complete set of isoclinic patterns is shown in figs. 12-25.

Stress patterns were also recorded on tracing paper. Full and half fringes were obtained by using dark and light fields respectively, and an estimation of quarter and three-quarter fringes was also made. Because the applied load varied for each model tested, no direct comparison could be made, but a few typical patterns are shown in figs. 10 and 11. To obtain accurately the fringe order in the corners, a method similar to that described in Ref. 2 (page 103) was used, the fringe being viewed through a low powered microscope. This technique was also applied to a limited extent along the free edge. The signs of the stresses along the free edge were determined by means of a tension compensation, by the method described in Ref. 3 (page 175).

4. Results

4.1. Peak shear stresses

The peak shear stress, which occurs at the intersection of the boom with the free edge, was determined from the expression $\tau = nF \sin 2\theta$ and the results expressed as $\frac{\tau}{\hat{\sigma}}$ are plotted against wedge angle in fig. 4.

4.2. Stress along the free edge

The direct stress along the free edge was found by the expression $\sigma_E = nF$, and plotted as $\sigma_E/\hat{\sigma}$ for various angles of sweep in figs. 5-9.

4.3. Signs of free edge stress

It was found by an inspection of the isoclinics, that a singular point existed on the free edge for all angles of sweep. Singular points are associated with a change in sign of boundary stress, and this is confirmed by the stress trajectories figs.26-39, which show that the lines of principal stress parallel to the edge change from the p type to the orthogonal q type at this point.

Figs. 26-39 also show that near corners where $\alpha < 90^\circ$, stress trajectories which originate normal to the boom are normal on intersection with the free edge. Since the boom is in tension the free edge stress must therefore also be tension for this region.

/By a ...

By a similar argument the free edge stress near a corner where $\alpha > 90^{\circ}$ may be shown to be compression. These results are confirmed by identifying boundary stresses using a tension compensation, which is an absolute method, in that it does not require the knowledge of the p or q stresses at a point on the model.

At the free edge - boom intersection, the isoclinics show that for corners where $\alpha < 90^{\circ}$, the parameters agree with the boundary conditions, but for $\alpha > 90^{\circ}$ this is not so, and therefore a singular point exists. Although a zero fringe cannot be seen in these corners, the presence of the singular point, and the fact that the sign of the boundary stress must change to agree with conditions for the boom, makes it reasonable to assume that a zero fringe does exist on the free edge.

The results obtained for the model with one boom were found to be similar to those for two booms, for the regions in the vicinity of the corners. This check was performed to indicate whether or not the two boom specimens were of satisfactory dimensions to prevent interaction of one half with the other. It was also made, as referred to later, to compare with certain results obtained by Palmer (Ref. 4).

5. Discussion of Results

The models under test in this thesis differed from the idealised structure considered by Mansfield in his theoretical work Ref. 1 in one important aspect, in that the flexural rigidity of the booms may not be considered negligible. This inconsistency may well have considerable effect, but the influence of this flexural rigidity may have been minimised if the method of loading the edge members had been modified, so that the bending moment on intersection with the web plate could be made zero. The value of such a modification would be that the theoretical assumptions would be fulfilled more completely, but the loading actually used in the tests was similar to that which would be applied in practical problems, such as an undercarriage cut-out in a wing panel, where bending of booms may take place.

The fact that it was impossible to design constant stress booms is not an important one. It is seen from Ref. 1 (Appendix I) that "the stress distribution in the immediate vicinity of the apex of a wedge is independent of the boundary conditions away from the apex", and so the peak values of the shear stress, on the free edge at the apex, should be the same for both constant stress and constant area booms. The distribution of the stresses near the apex however

/cannot be ...

cannot be checked, because the values of $\frac{2\sigma}{\partial r}$ and $\frac{2\tau}{\partial r}$ are given to be zero only when the main members have constant stress characteristics.

5.1. Peak shear stress

The peak values of the shear stress shown in fig. 4, are in fairly good agreement with theory for $\alpha < 90^{\circ}$, and when it is considered that the equation is not valid for $\alpha = 129^{\circ}$, and that high shear stresses are predicted for $\alpha > 120^{\circ}$, experimental results are in reasonable agreement for large values of α .

The results show that for $\alpha = 130^{\circ}$ the peak shear stress is almost twice that for $\alpha = 90^{\circ}$, while for $\alpha = 50^{\circ}$, it is just over one half. Angles of sweep of this order are quite common in modern design, and shear stresses may be seriously underestimated, or overestimated if no account is made of the effects of sweep, both conditions resulting in an unsatisfactory design.

L.H. Mitchell in Ref. 4, investigated the diffusion problem in unswept panels by means of photoelasticity, and the results obtained provide a useful check for $\alpha = 90^{\circ}$. For the model most similar to the ones considered in this thesis, the ratio $\frac{\pi}{2} \cdot \frac{\tau}{\hat{\sigma}}$ was found to be 0.80, which gives $\frac{\tau}{\hat{\sigma}} = 0.59$. This agrees with the value given for $\alpha = 90^{\circ}$ in fig. 4, to within 10%.

5.2. Stress along the free edge

Considering the expression given by Mansfield for the direct stress at the apex, it is seen that when $\alpha = 129^{\circ}$ the shear stress becomes infinite, and for $\alpha > 129^{\circ}$ the sign of the direct stress changes in a similar manner to the shear stress. Hence it is reasonable to assume that this equation also becomes invalid for $\alpha = 129^{\circ}$, and that stresses should be high but do not change their sense for $\alpha > 129^{\circ}$. The experimental results then show reasonable agreement for $\alpha > 90^{\circ}$. For $\alpha = 90^{\circ}$ the stress ratio $\sigma_E/\hat{\sigma}$ is -0.55 compared with -1.0 given by theory, and as α is increased the stress ratio becomes larger, until at $\alpha = 150^{\circ}$ it has reached a value of -1.63.

For values of α less than 90°, fig. 5 shows that the edge stress changes its sense, and then increases to a large positive value, whereas the theoretical solution gives small values of the oposite sign. It therefore seems likely that the theoretical solution is at fault for these small values of α , especially when it is considered that when $\alpha = 0$ is substituted

/in the ...

in the equation, the stress ratio becomes zero, whereas unity seems a more likely value.

The direct stress away from the corners was relatively easy to measure, and the results are probably more accurate than those obtained in the immediate vicinity of the corners. This is because the stresses do not vary so rapidly. Therefore these stress distributions may supply a boundary condition for a solution by relaxation methods, and as the distributions for constant stress booms may not differ very much, they may be used as a first approximation for this case also.

5.3. Previous experimental work

Ref. 4 gives the results of a photoelastic investigation into the problems discussed in this thesis, using models cast in Marco resin, and having only one boom. The conclusions drawn from these tests do not compare favourably with this present work, and possible reasons for discrepancies are suggested.

The first fundamental difference can be found in the diagrams of stress trajectories. Ref. 4 shows them to be very similar for all angles of sweep, whilst figs. 26-37 show that the type of patterns obtained differ considerably when the angle of sweep is varied. Because of this discrepancy, the model with only one boom was made, and the stress trajectories for this model, shown in figs. 38 and 39 show that, in the vicinity of the corners, the type of patterns obtained is the same as for the two boom model, with the same sweep. Unfortunately Ref. 4 does not show the isoclinics from which the trajectories were obtained, and so no further comparisons can be made.

The effect of the differences shown above is that in Ref. 4 the free edge stress is given to be always tension, for all angles of sweep.

Another interesting comparison can be made between the fringe patterns. For $\alpha = 60^{\circ}$, fig. 11 shows a zero fringe about 0.3in. from the corner, and although for the corresponding angle in Ref. 4 (Fig. 14) the pattern is very obscure, a zero fringe does seem apparent at $\alpha = 30^{\circ}$. However a zero stress is never recorded in the results for any angle of sweep.

It must also be remarked that the observation that "the theoretical assumption that the stress distribution in the wedge is constant along radial lines is not justified by experiment", is inaccurate. This is because the models used in the test did not satisfy the condition that the main members should have constant stress characteristics.

/6. ...

6. Conclusions

Peak shear stresses found experimentally were found to agree with the prediction of Mansfield, in that for large values of the wedge angle, the stresses were considerably greater than for the case with no sweep, and for small angles the stresses were smaller - the ratio $\frac{\tau}{\sigma}$ being 0.98 and 0.3 for $\alpha = 130^\circ$ and 50° respectively, compared with 0.5 for $\alpha = 90^\circ$.

The values obtained for direct stress in the free edge at the apex of the wedge, show that the theoretical solution becomes invalid for $\alpha = 129^\circ$, and for $\alpha > 129^\circ$, the stresses do not change their sense, but become large. For $\alpha > 90^\circ$ the stresses were of opposite sign and of much greater magnitude than for $\alpha < 90^\circ$.

References

No.	Author	Title, etc.
1.	E.H. Mansfield	Stress concentrations at a cut-out in a swept wing. R.A.E. Report Structures 114.
2.	R.B. Heywood	Design by photoelasticity. 1952. Chapman and Hall.
3.	M.M. Frocht	Photoelasticity Vol. I. 1941. John Wiley and Sons.
4.	P.J. Palmer	A photoelastic investigation into the stress concentrations in a panel bounded by a main load carrying member and an oblique edge. A.R.C. Report Strut. 1592.

FIG. 1.

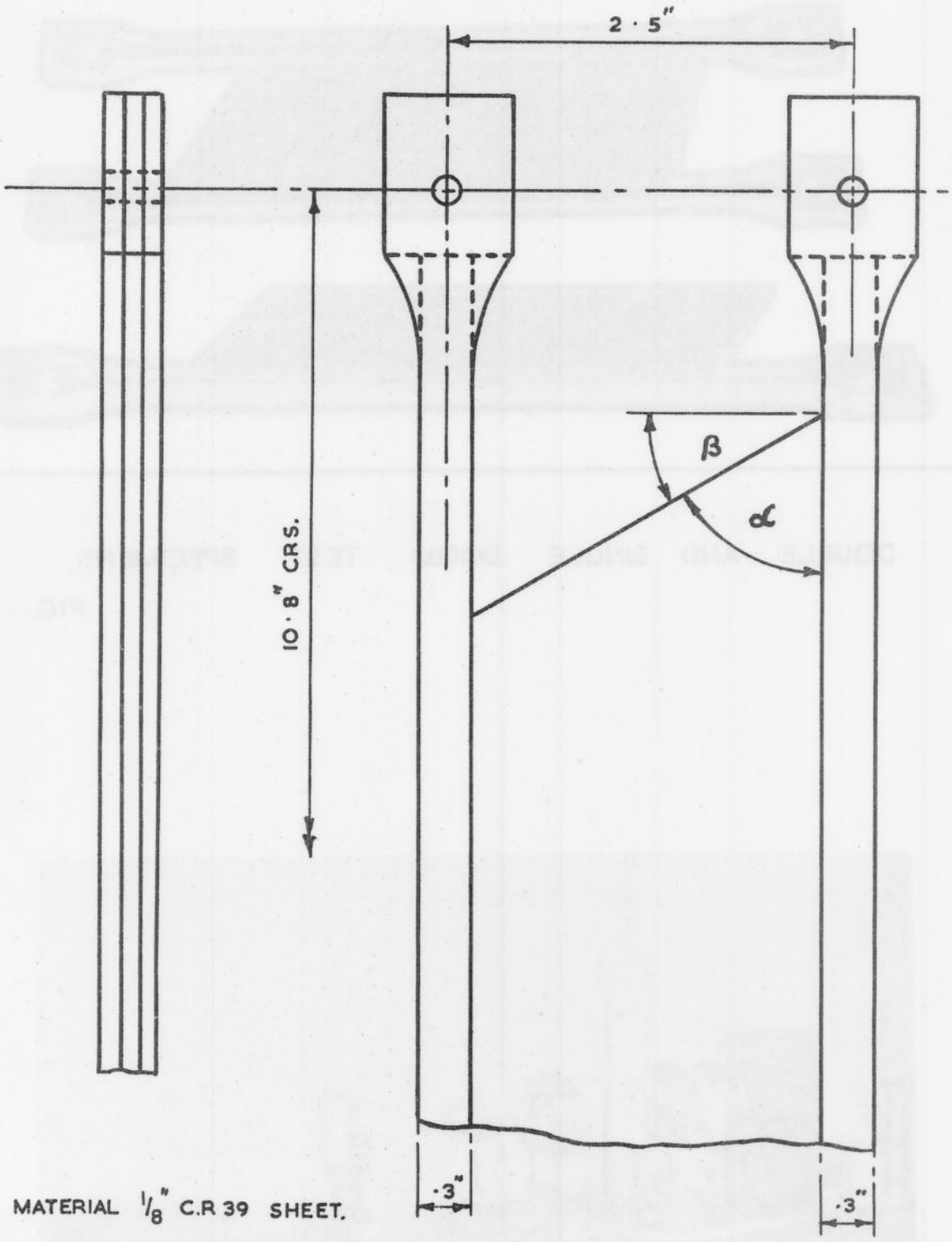

TEST SPECIMEN DIMENSIONS

FIGS. 2 & 3.

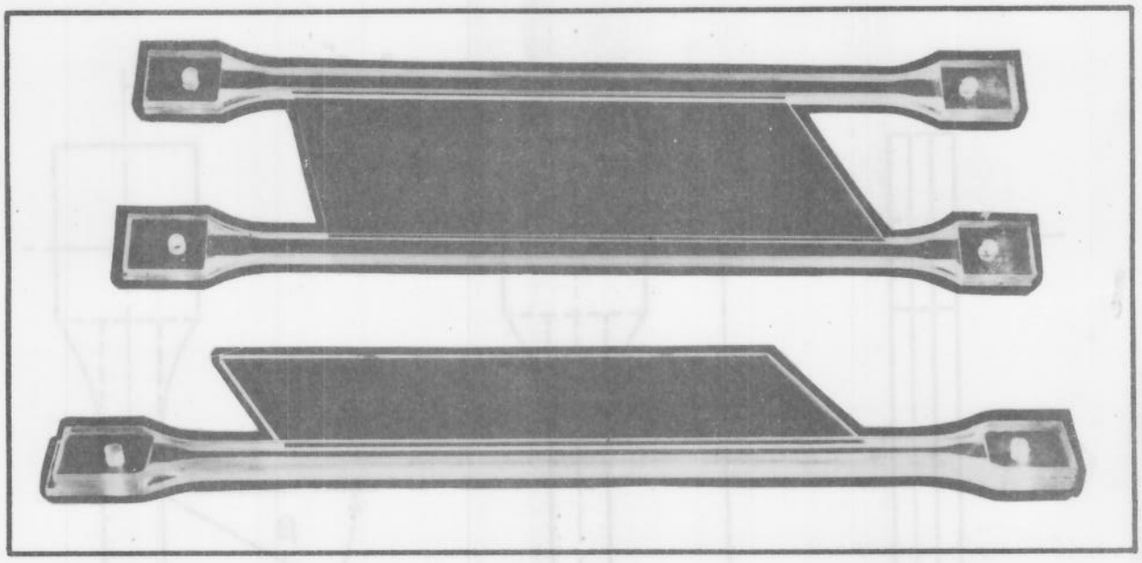

DOUBLE AND SINGLE BOOM TEST SPECIMENS

FIG. 2.

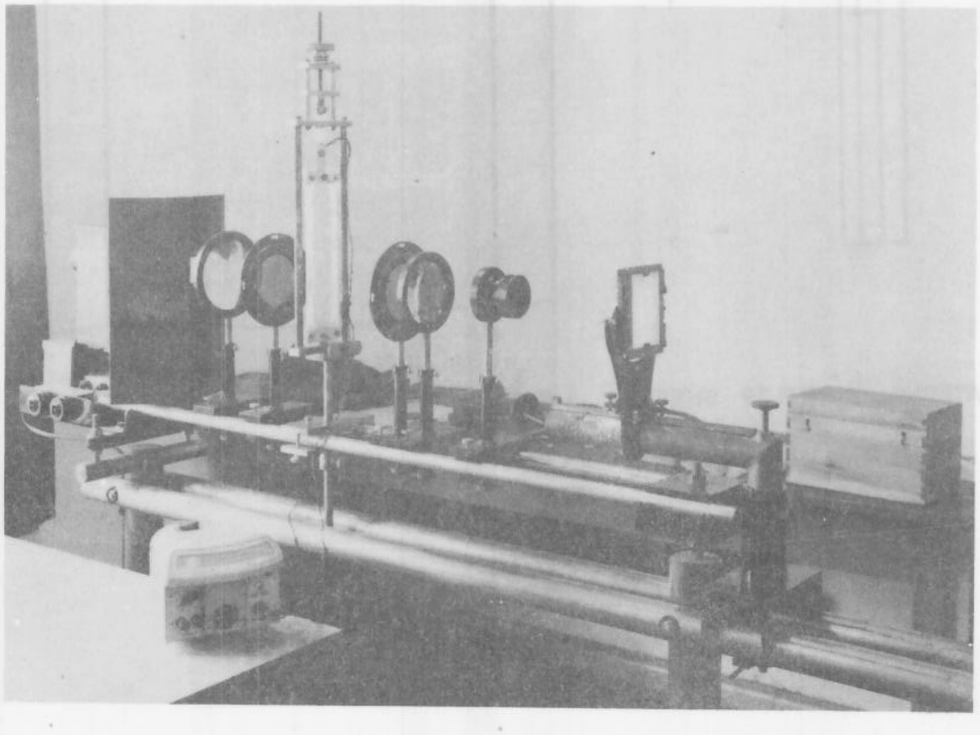

THE POLARISCOPE AND LOADING APPARATUS

FIG. 3.

FIG. 4.

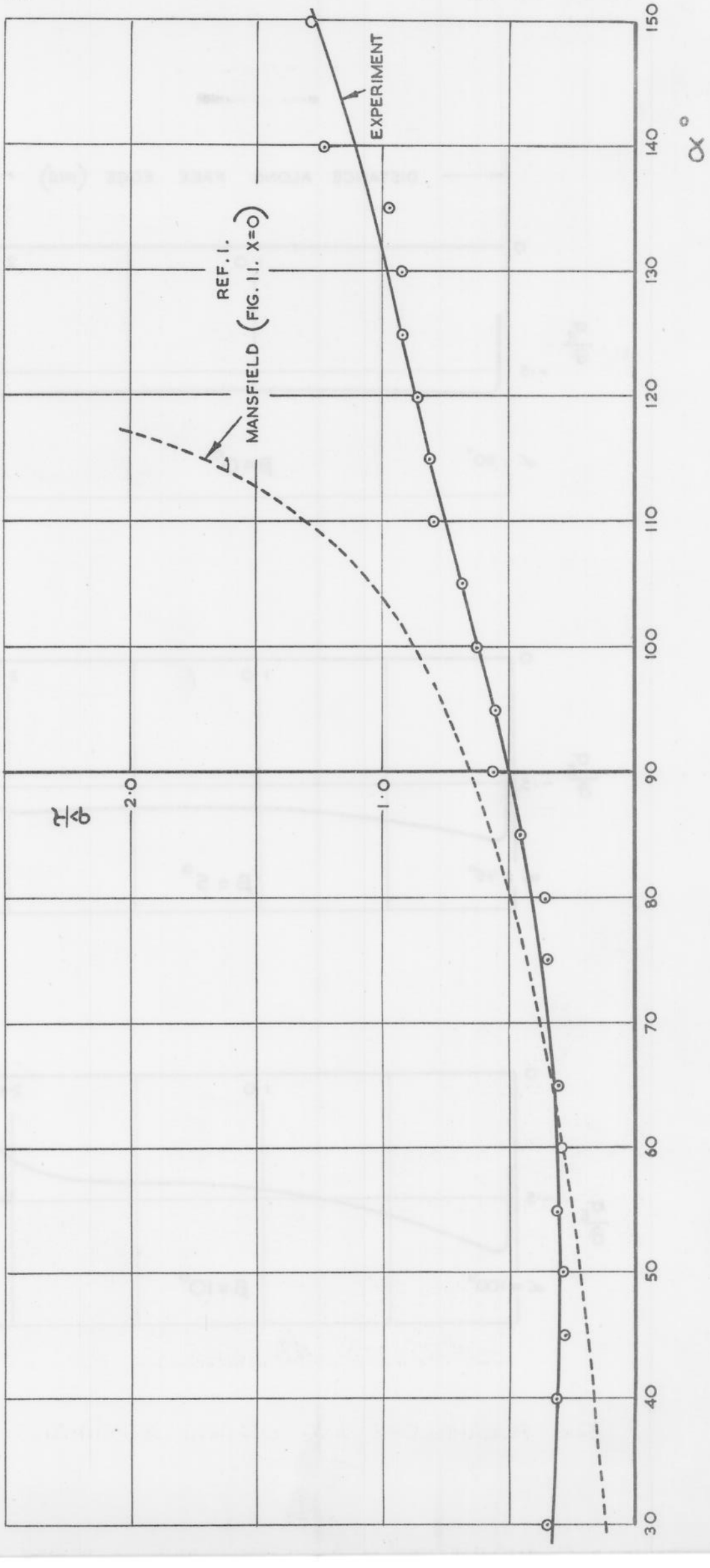
EXPERIMENT
REF. 1.
MANSFIELD (FIG. 11. X=0)
q/R
2·0
1·0
α°
150
140
130
120
110
100
90
80
70
60
50
40
30

FIG. 5.

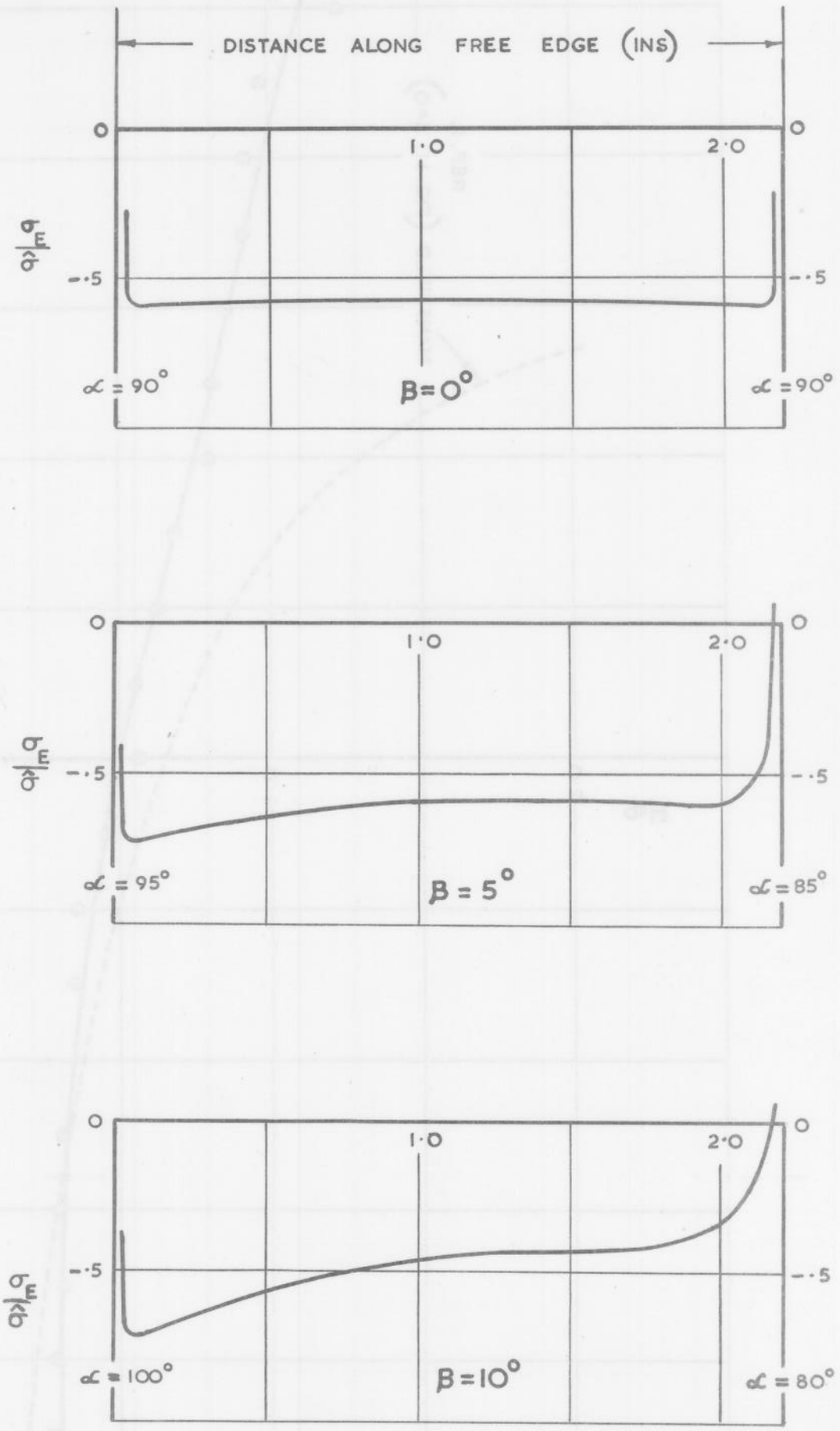
DISTANCE ALONG FREE EDGE (INS)
0
1·0
2·0
0
$\frac{q}{q_E}$
-·5
-·5
$\alpha = 90°$
$\beta = 0°$
$\alpha = 90°$
0
1·0
2·0
0
$\frac{q}{q_E}$
-·5
-·5
$\alpha = 95°$
$\beta = 5°$
$\alpha = 85°$
0
1·0
2·0
0
$\frac{q}{q_E}$
-·5
-·5
$\alpha = 100°$
$\beta = 10°$
$\alpha = 80°$

FIG. 6.

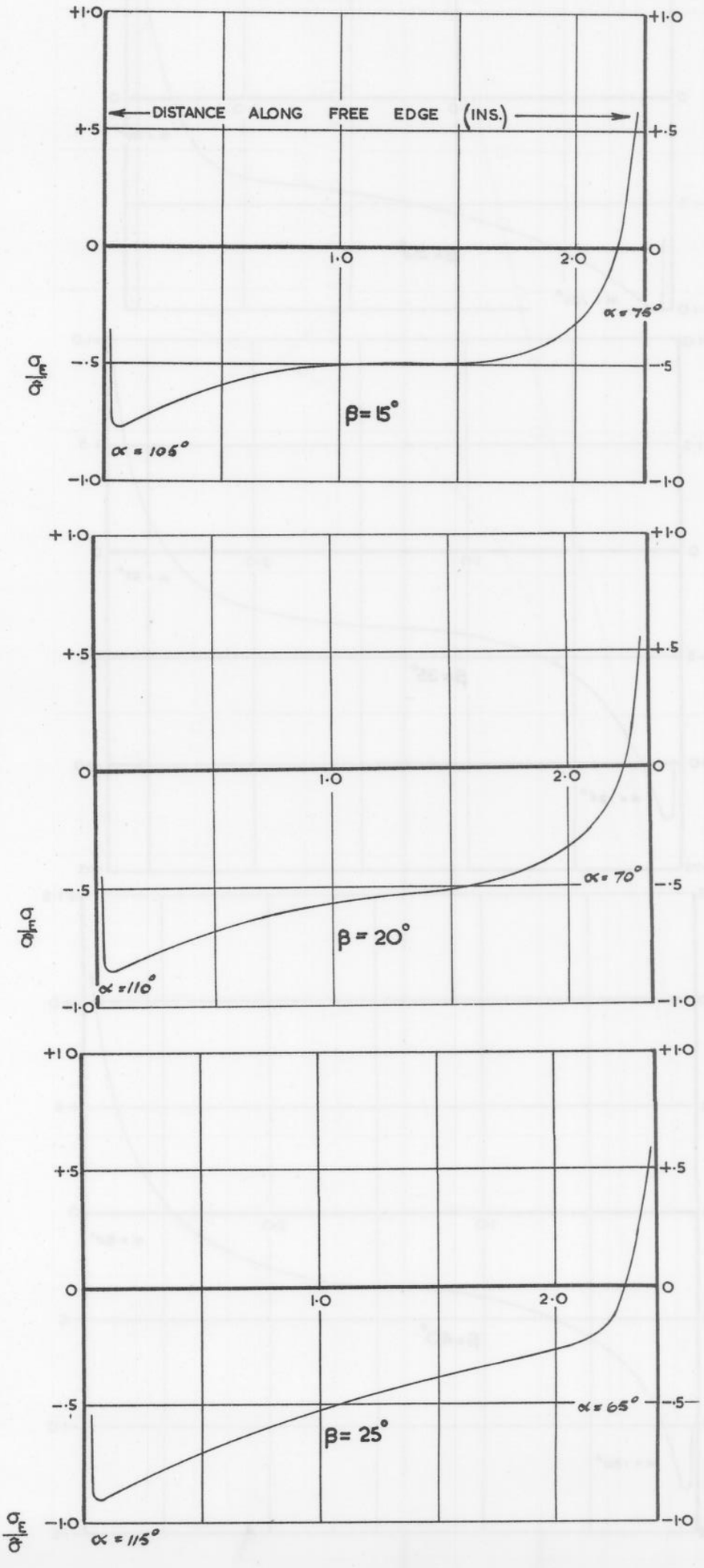
+1·0
+·5
0
−·5
−1·0
DISTANCE ALONG FREE EDGE (INS.)
1·0
2·0
α = 76°
β = 15°
α = 105°
α = 70°
β = 20°
α = 110°
α = 65°
β = 25°
α = 115°

COLLEGE OF AERONAUTICS

REPORT No. 78.

FIG. 7.

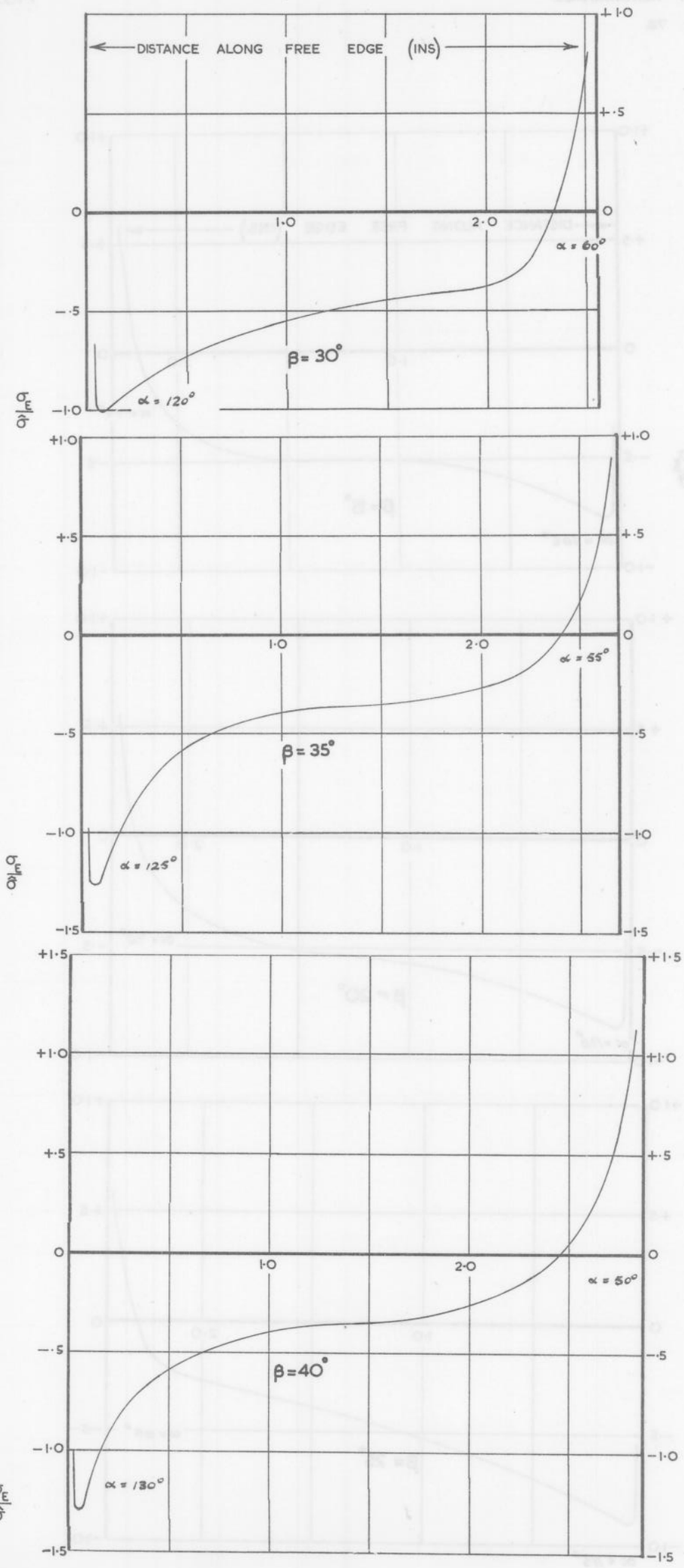

FIG. 8.

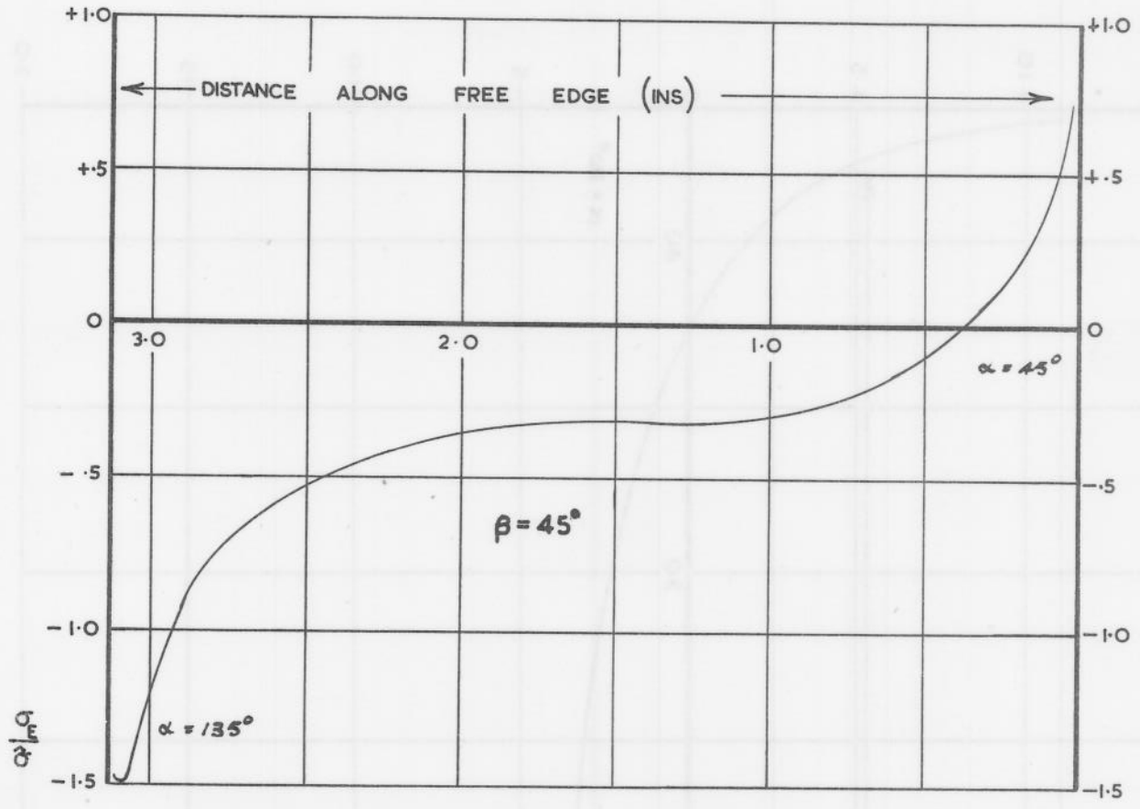
DISTANCE ALONG FREE EDGE (INS)
+1·0
+·5
0
−·5
−1·0
−1·5
3·0
2·0
1·0
α = 45°
β = 45°
α = 135°
σξ/σ

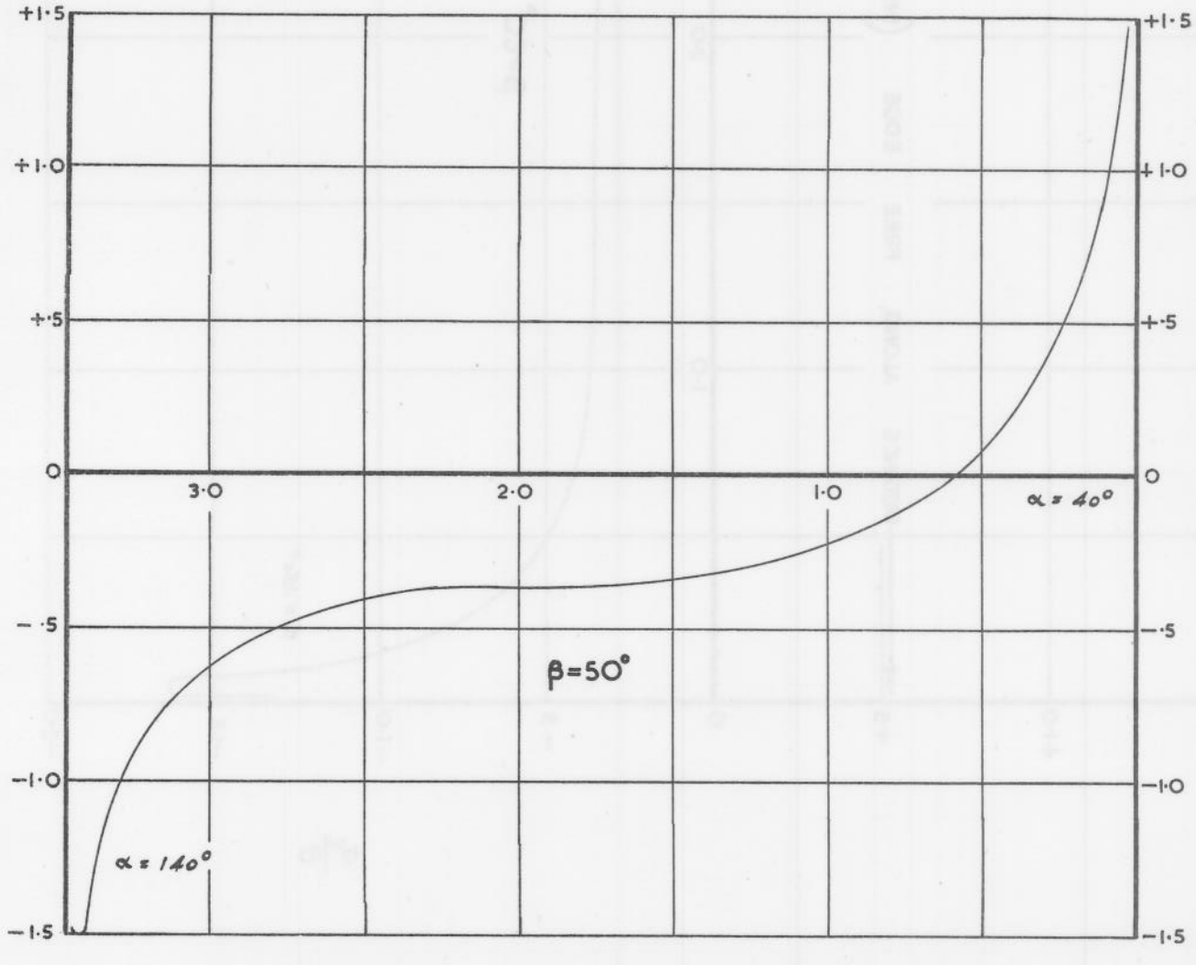
+1·5
+1·0
+·5
0
−·5
−1·0
−1·5
3·0
2·0
1·0
α = 40°
β = 50°
α = 140°
σξ/σ

COLLEGE OF AERONAUTICS

REPORT No. 78.

FIG. 9.

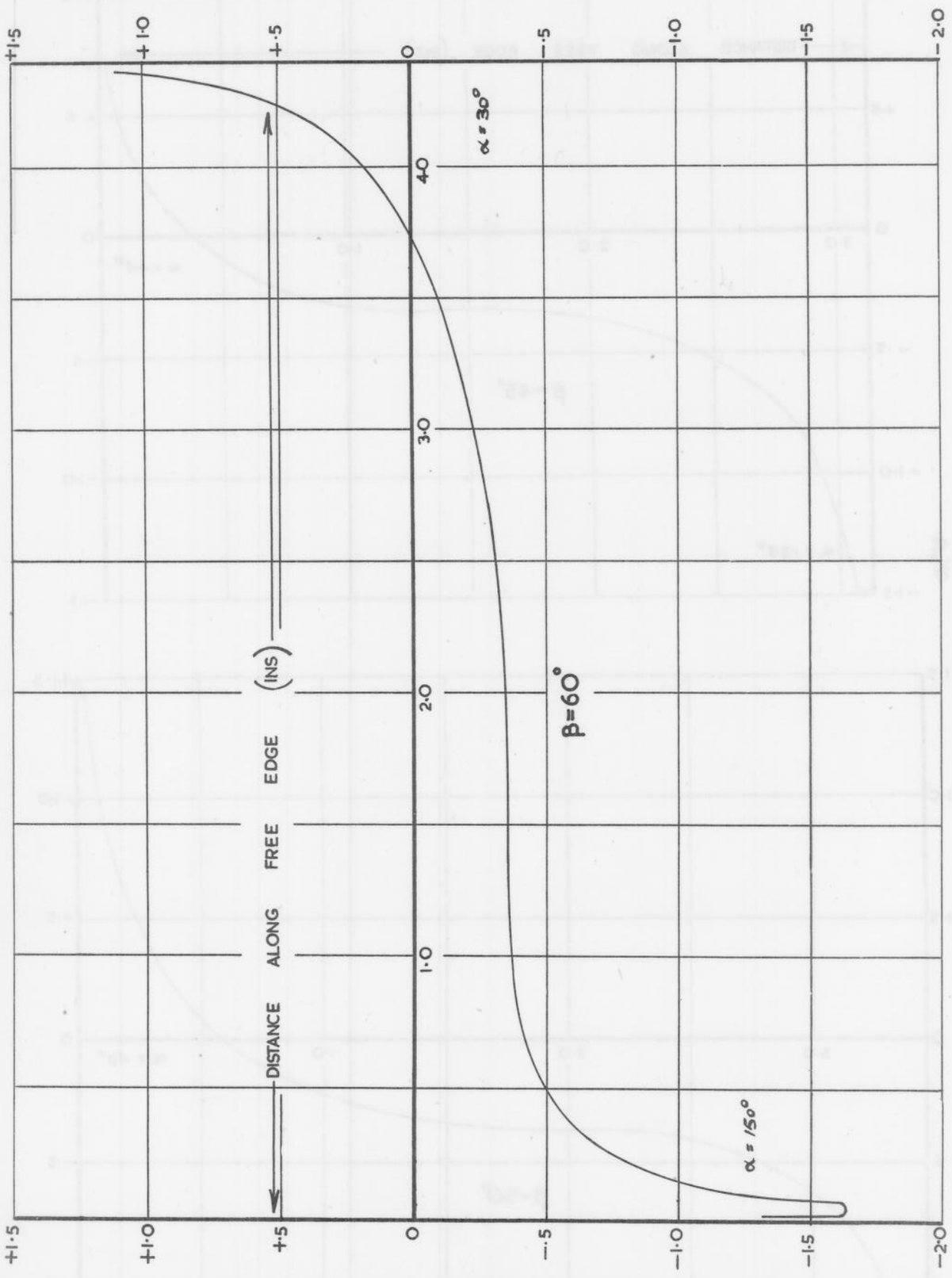

σ^E/σ

FIG. 10.

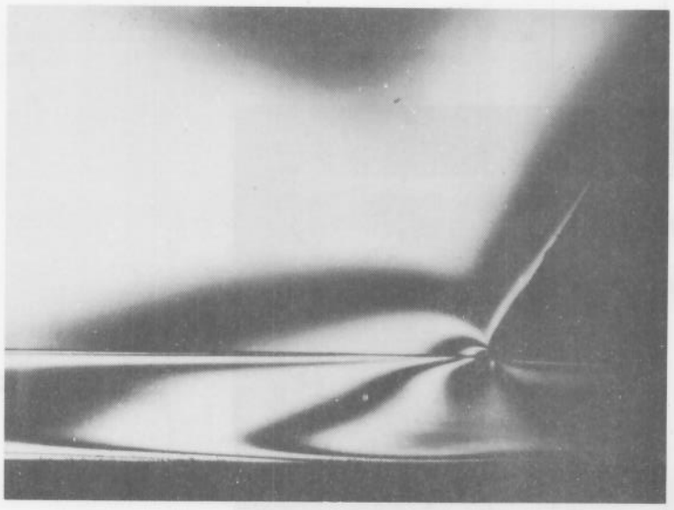

$\alpha = 120°$

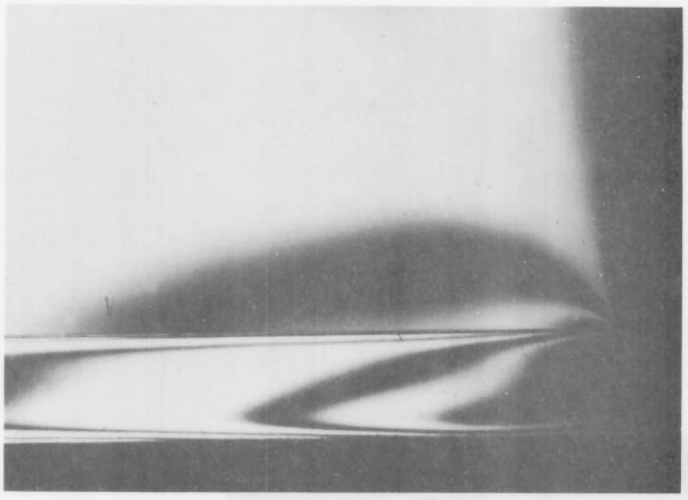

$\alpha = 90°$

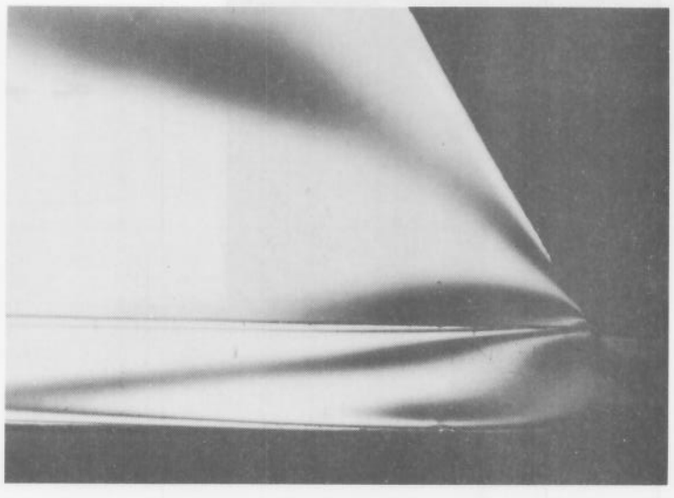

$\alpha = 60°$

FRINGES FOR MODELS WITH TWO BOOMS

FIG. 11.

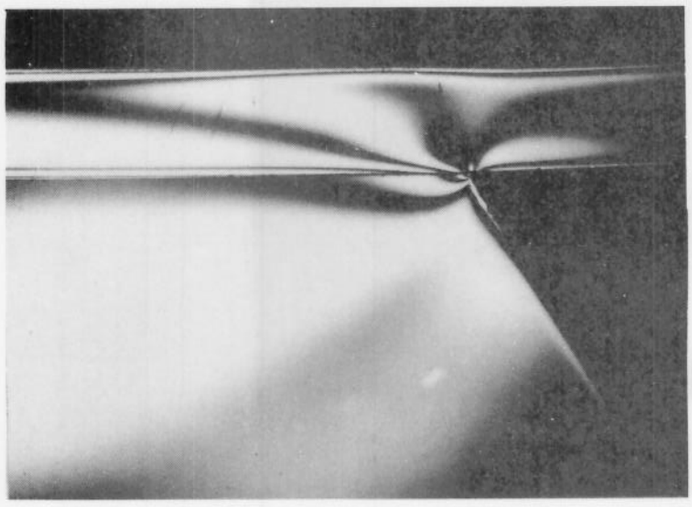

$\alpha = 120°$

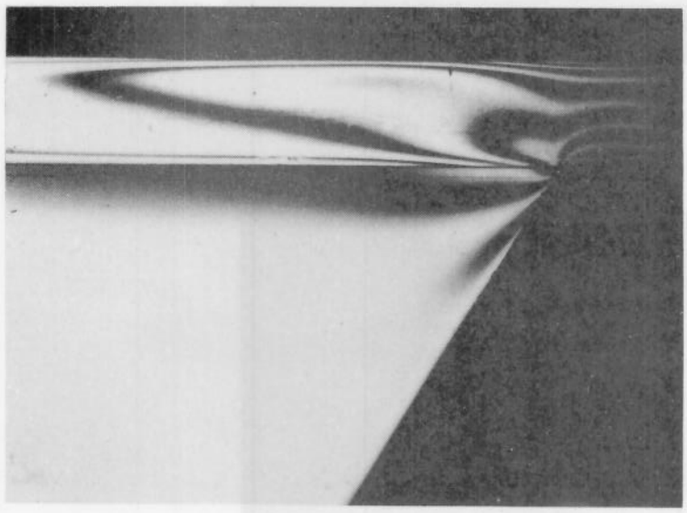

$\alpha = 60°$

FRINGES FOR MODELS WITH ONE BOOM

FIGS. 12, 13 & 14.

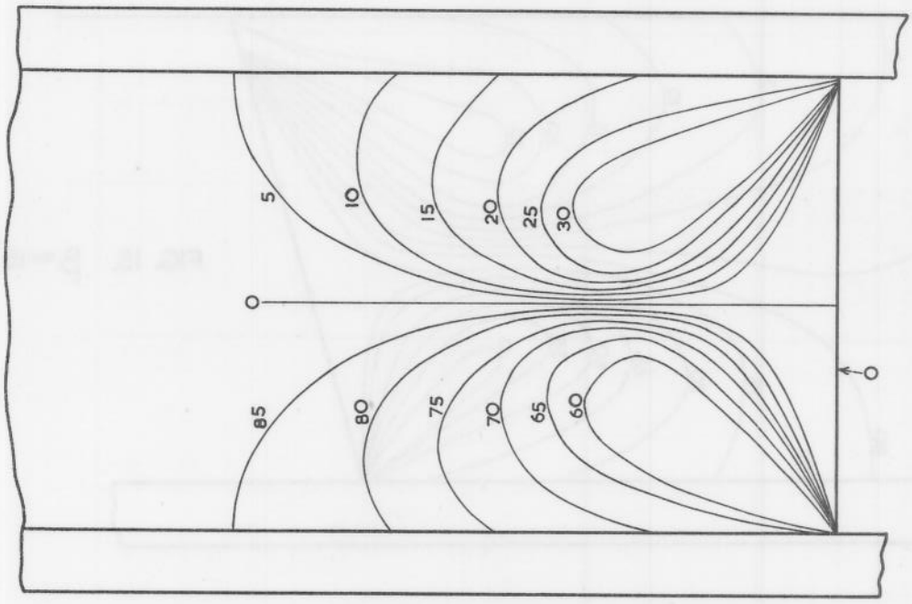

ISOCLINICS $\beta = 0^\circ$
FIG. 12.

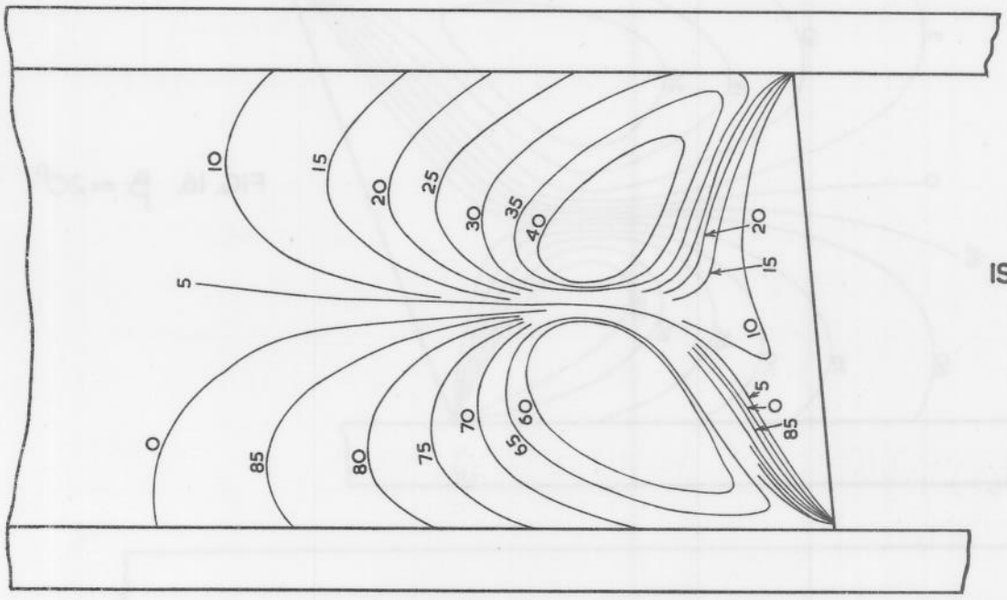

ISOCLINICS $\beta = 5^\circ$
FIG. 13.

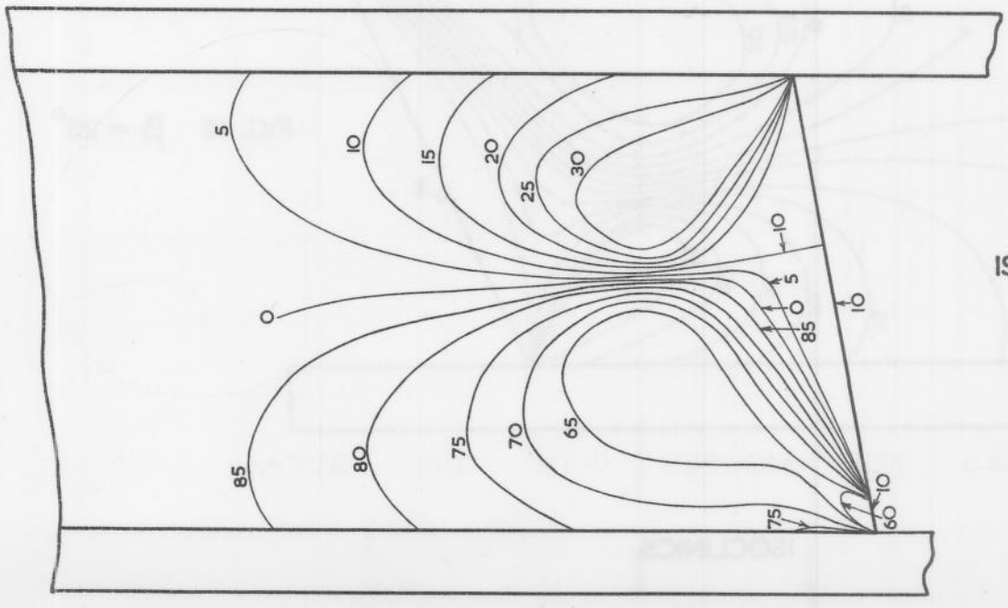

ISOCLINICS $\beta = 10^\circ$
FIG. 14.

FIGS. 15, 16 & 17.

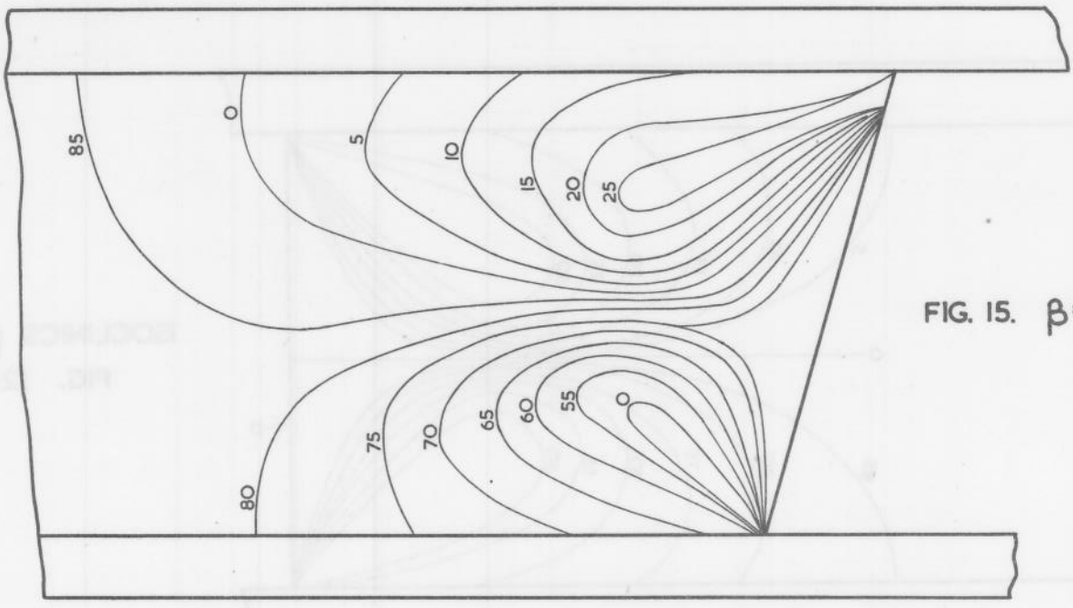

FIG. 15. $\beta = 15^\circ$

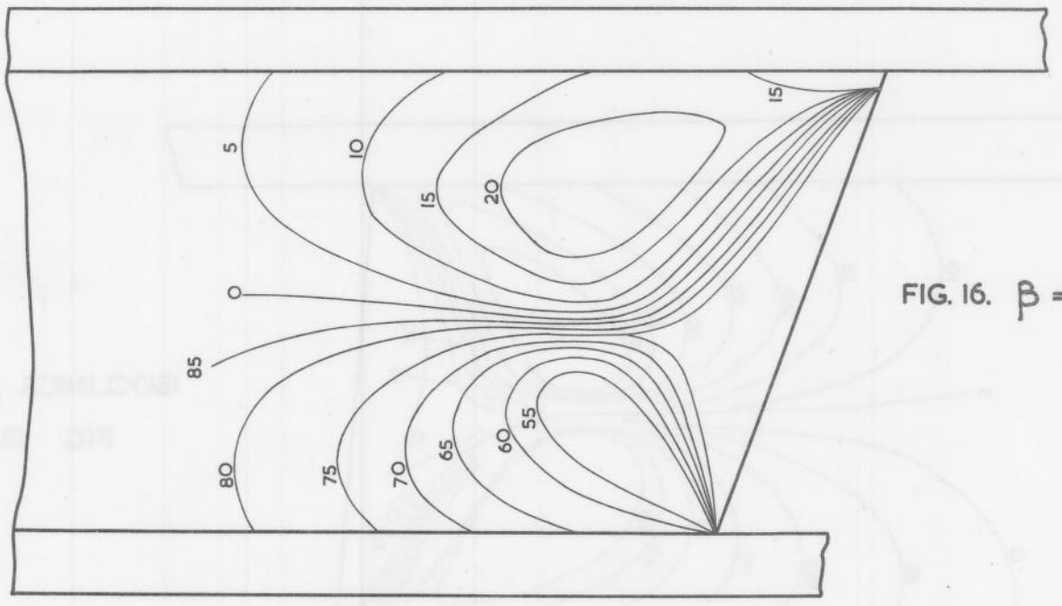

FIG. 16. $\beta = 20^\circ$

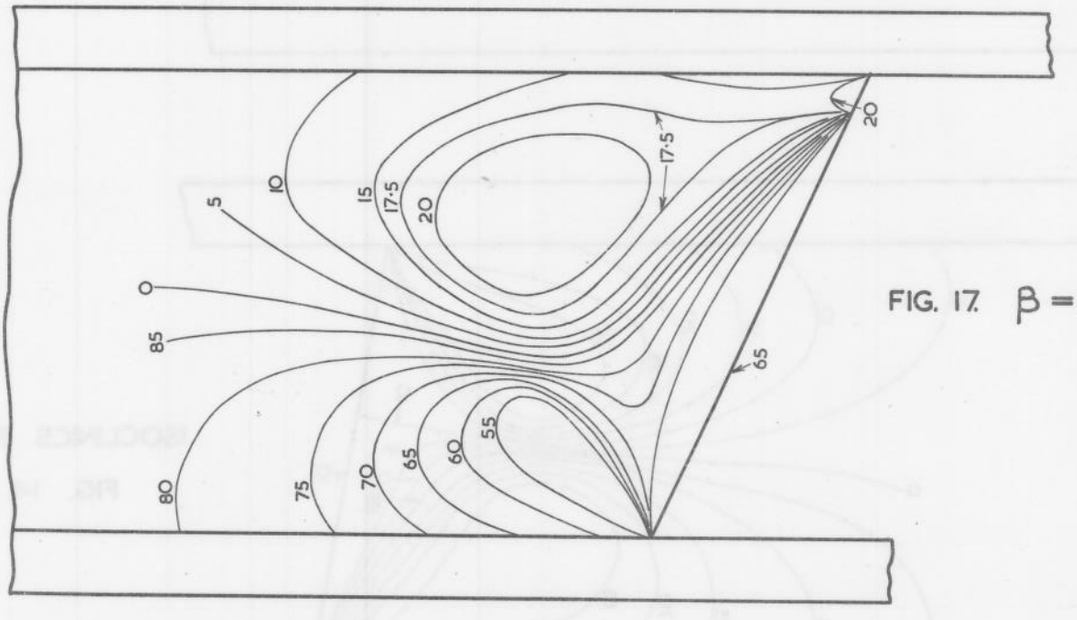

FIG. 17. $\beta = 25^\circ$

ISOCLINICS

FIGS. 18, 19 & 20.

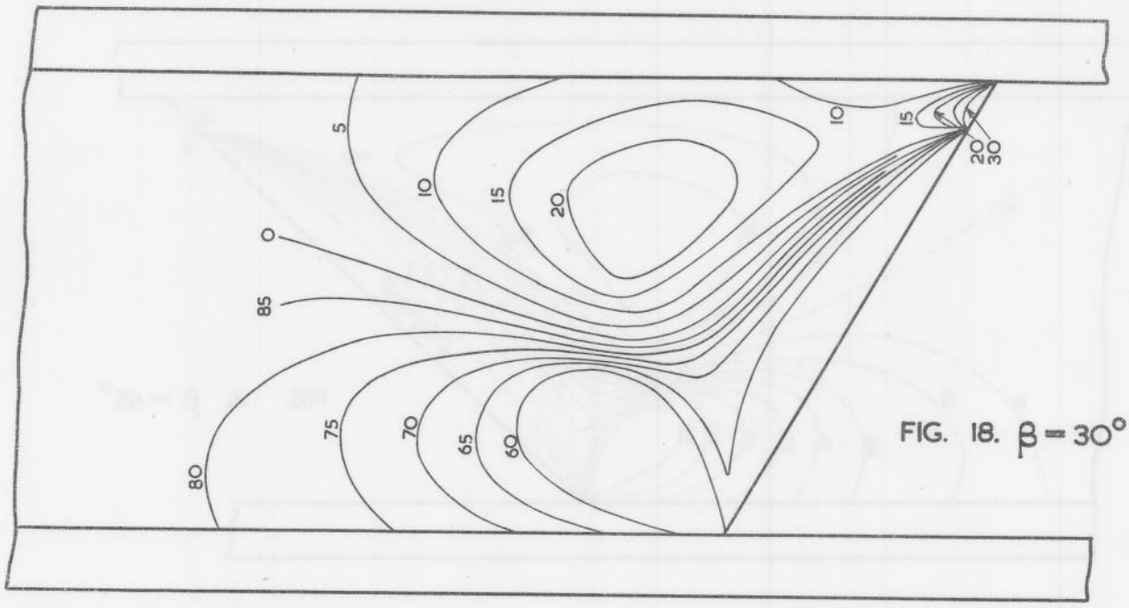

FIG. 18. $\beta = 30°$

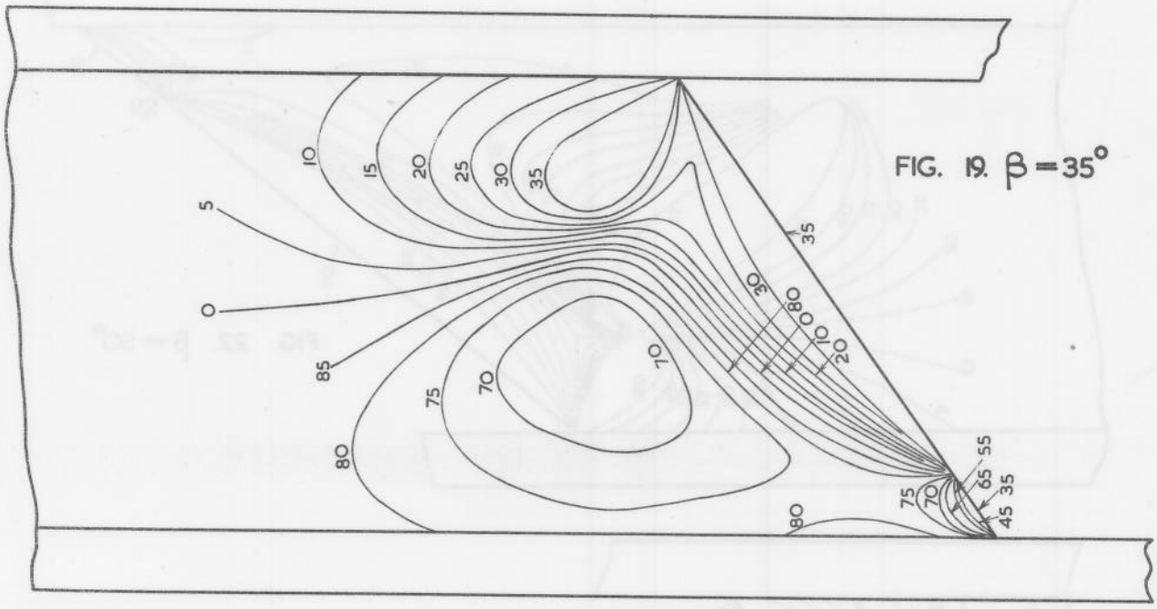

FIG. 19. $\beta = 35°$

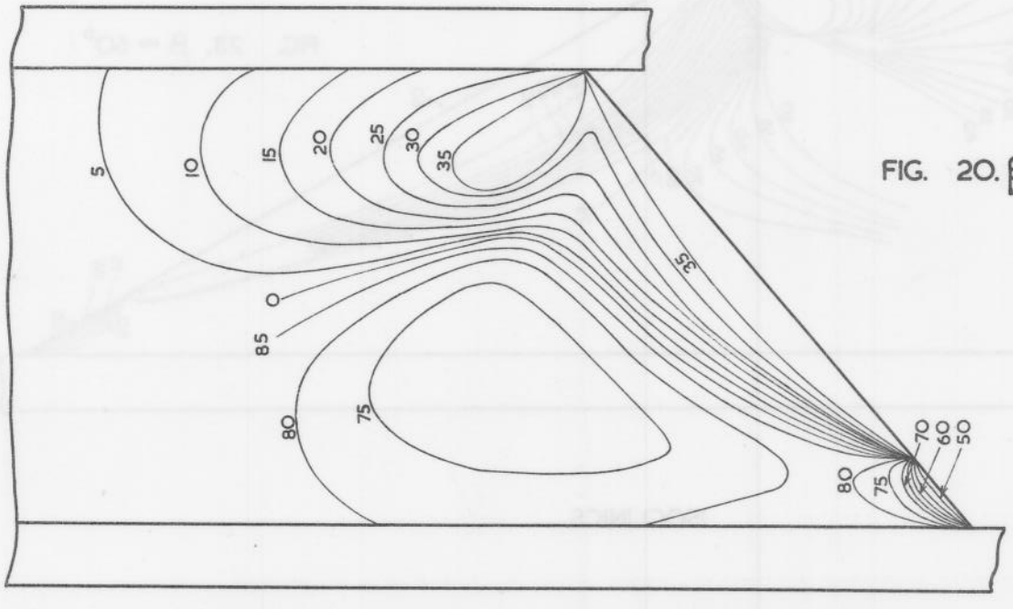

FIG. 20. $\beta = 40°$

ISOCLINICS

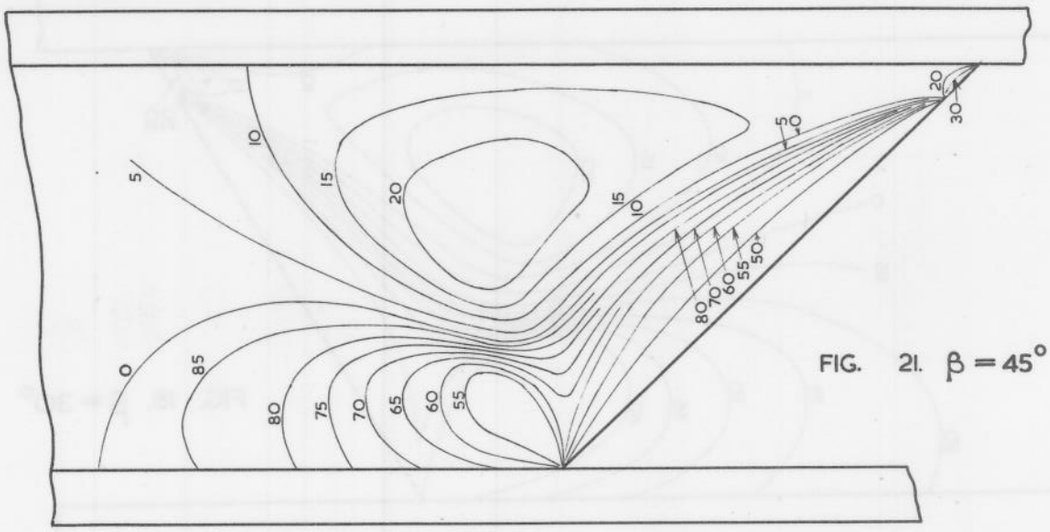

FIG. 21. $\beta = 45°$

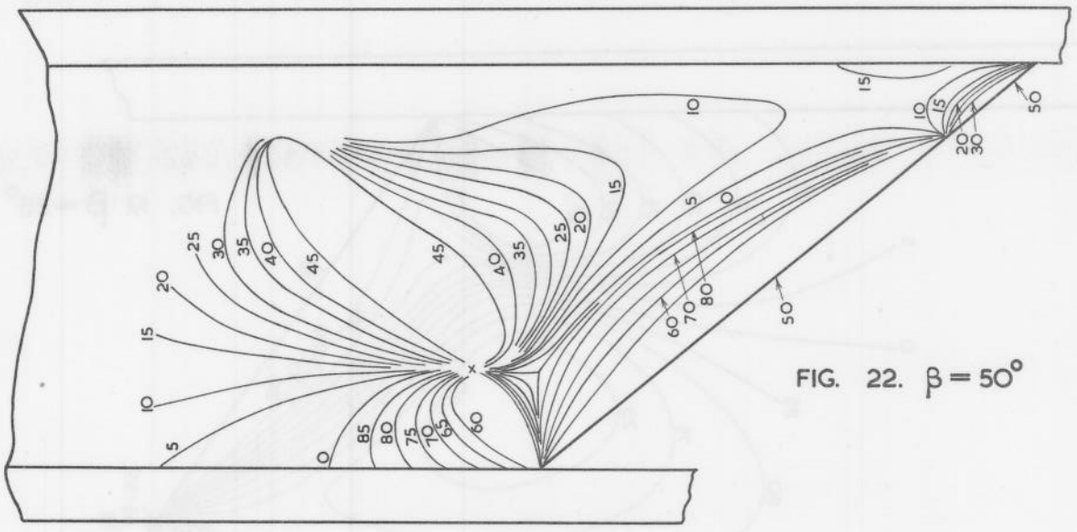

FIG. 22. $\beta = 50°$

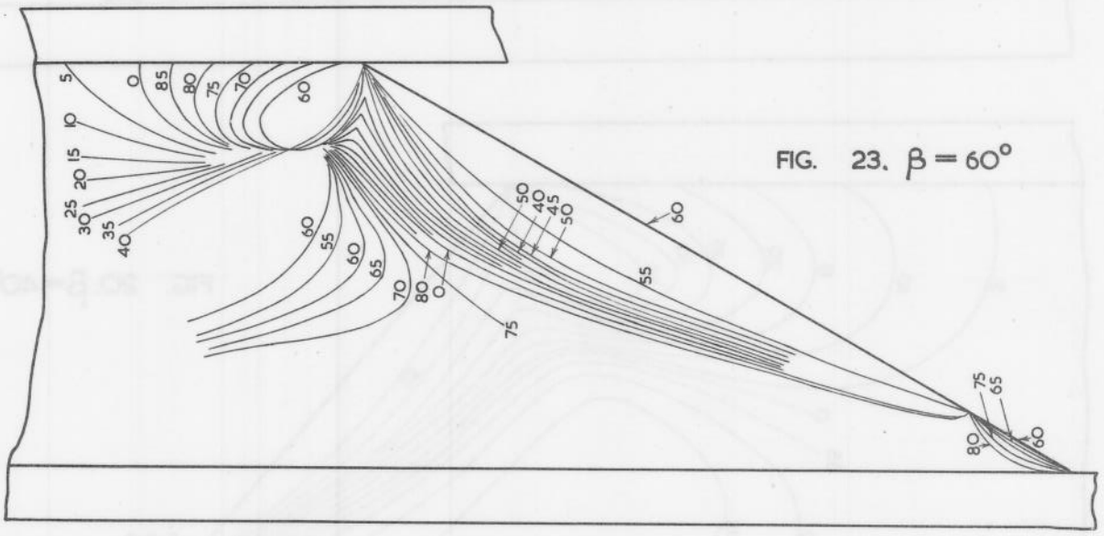

FIG. 23. $\beta = 60°$

ISOCLINICS

FIGS. 24 & 25.

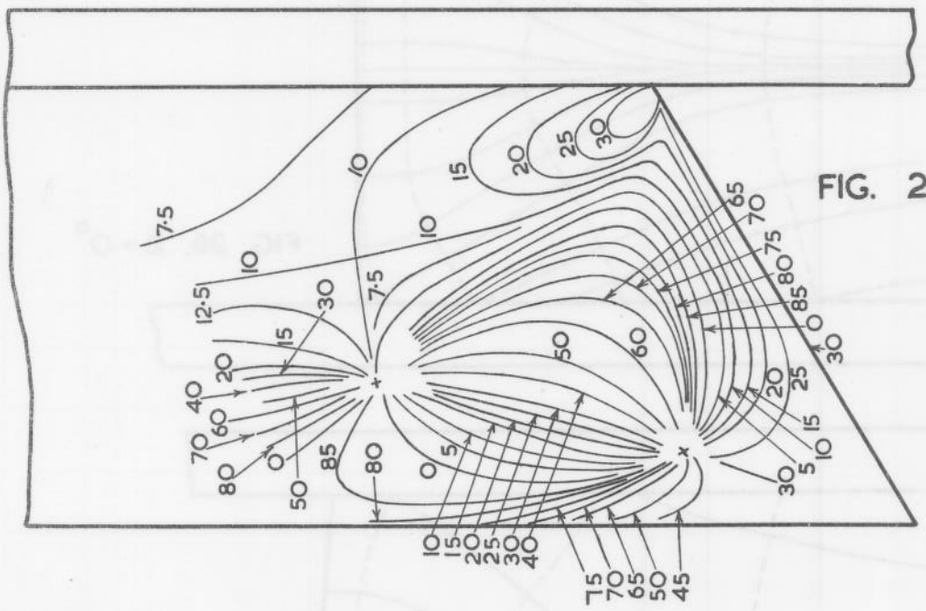

FIG. 24. $\beta = 30°$

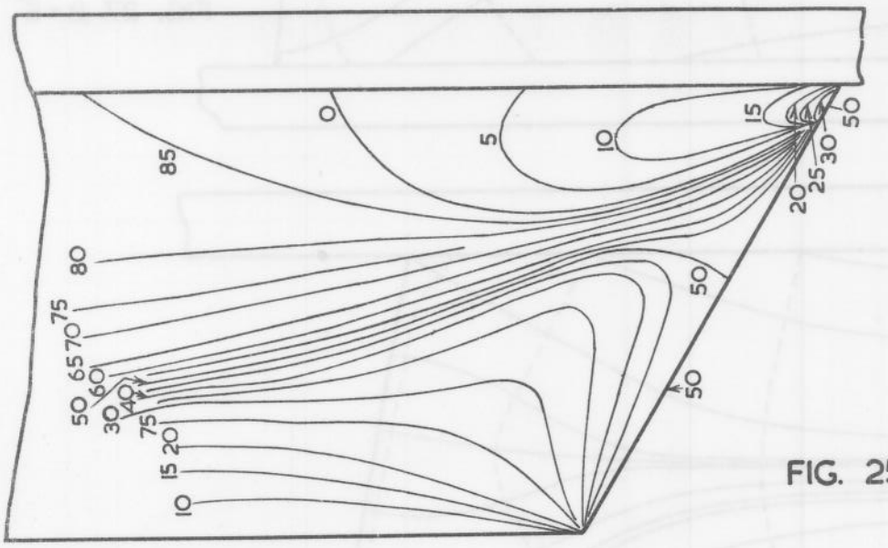

FIG. 25. $\beta = 30°$

ISOCLINICS SINGLE BOOM SPECIMEN

FIGS. 26. 27. & 28.

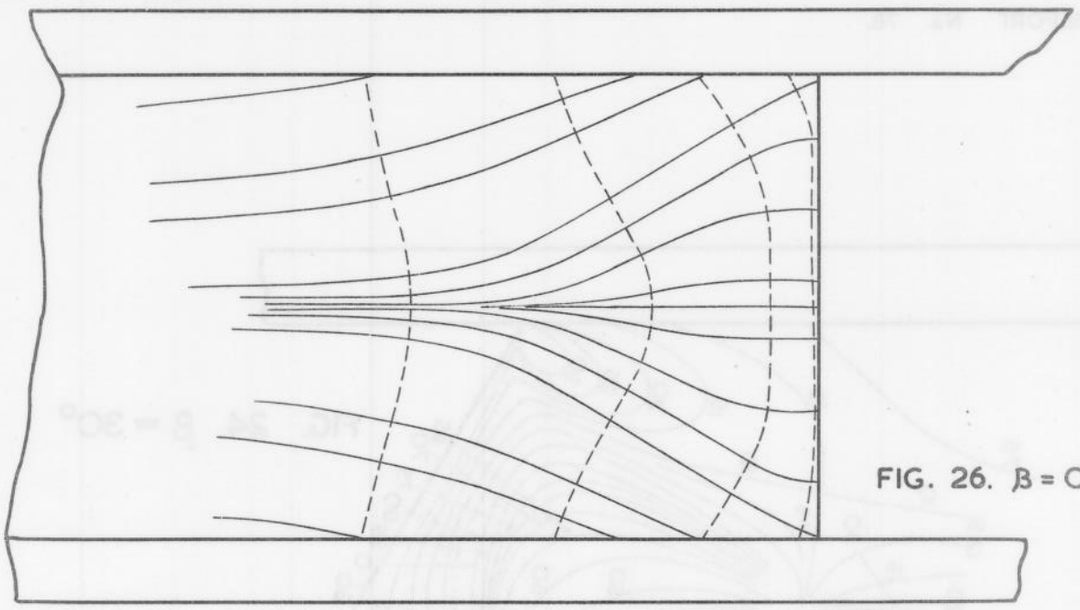

FIG. 26. $\beta = 0^\circ$

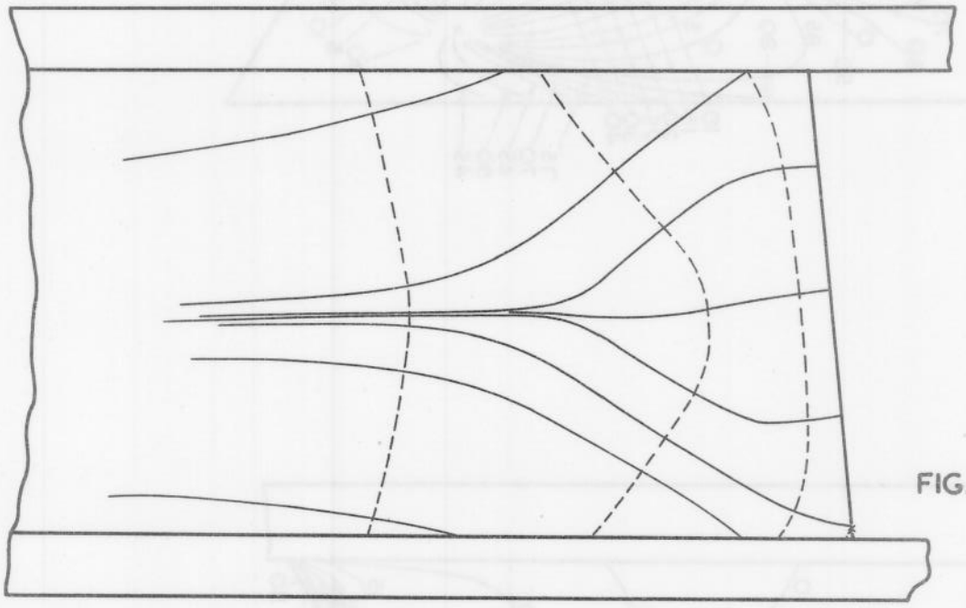

FIG. 27. $\beta = 5^\circ$

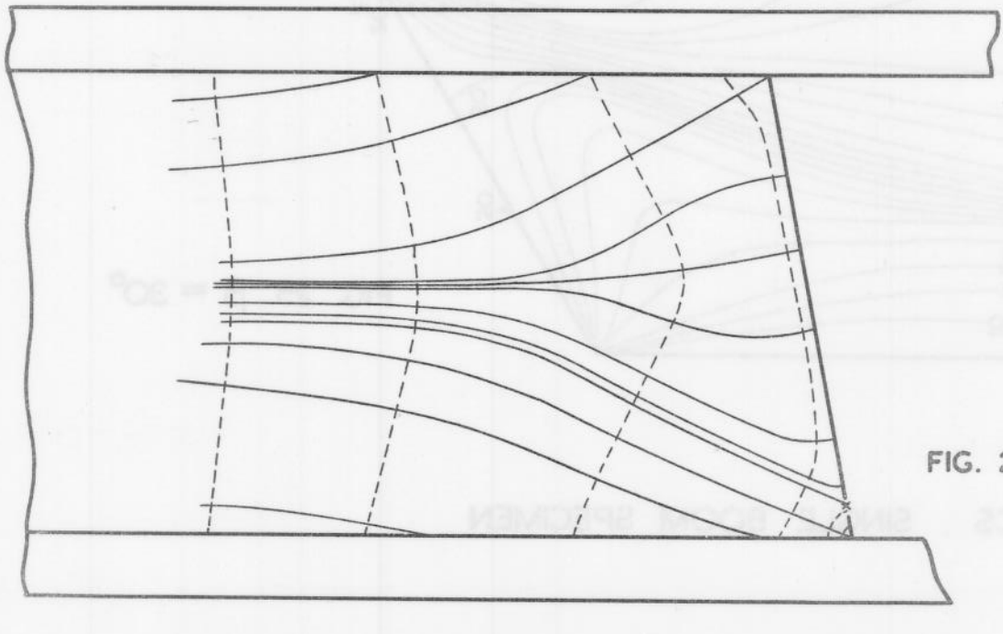

FIG. 28. $\beta = 10^\circ$

STRESS TRAJECTORIES

FIGS. 29, 30 & 31.

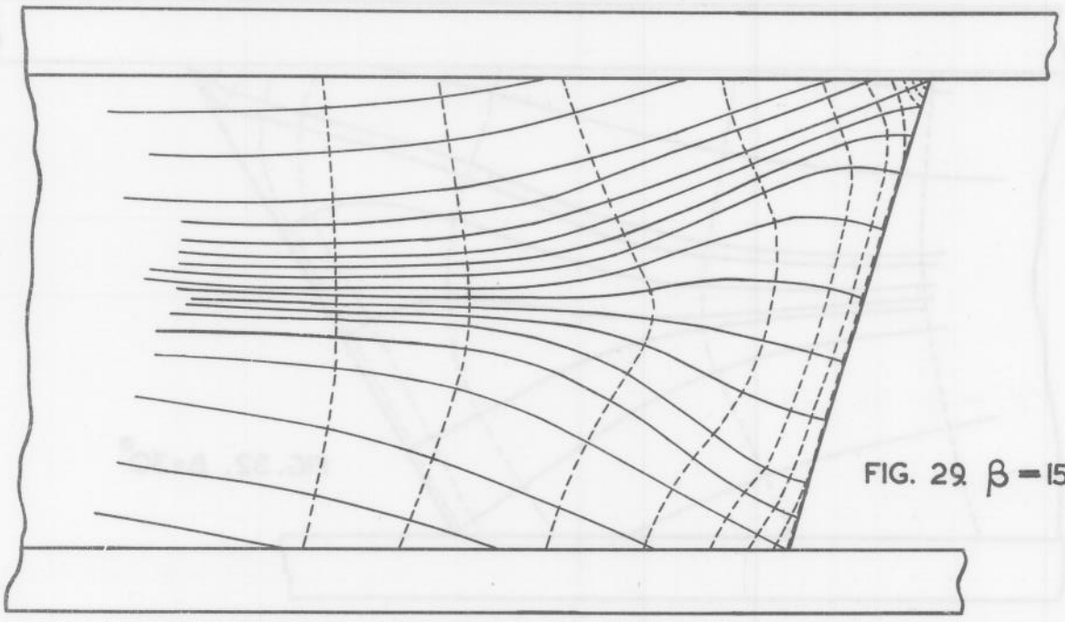

FIG. 29. $\beta = 15^{\circ}$

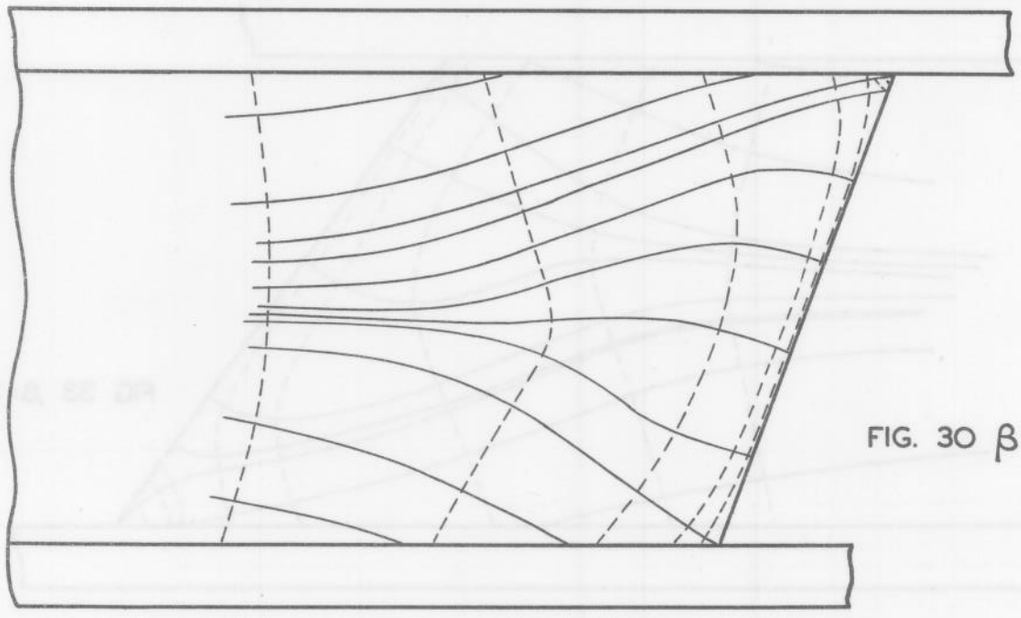

FIG. 30 $\beta = 20^{\circ}$

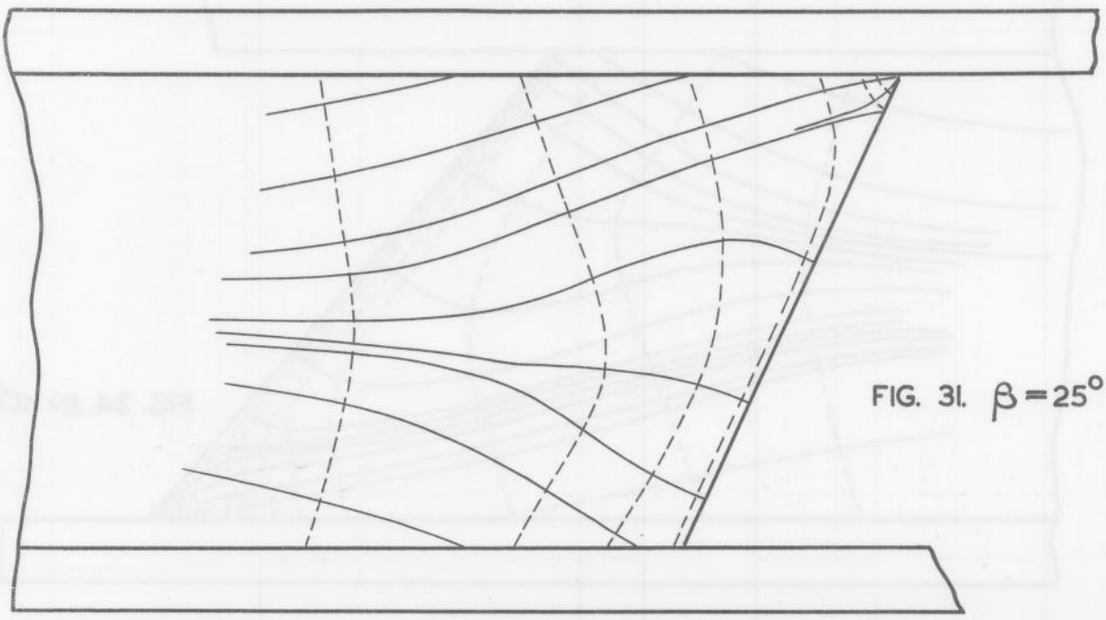

FIG. 31. $\beta = 25^{\circ}$

STRESS TRAJECTORIES

FIGS. 32,33 & 34

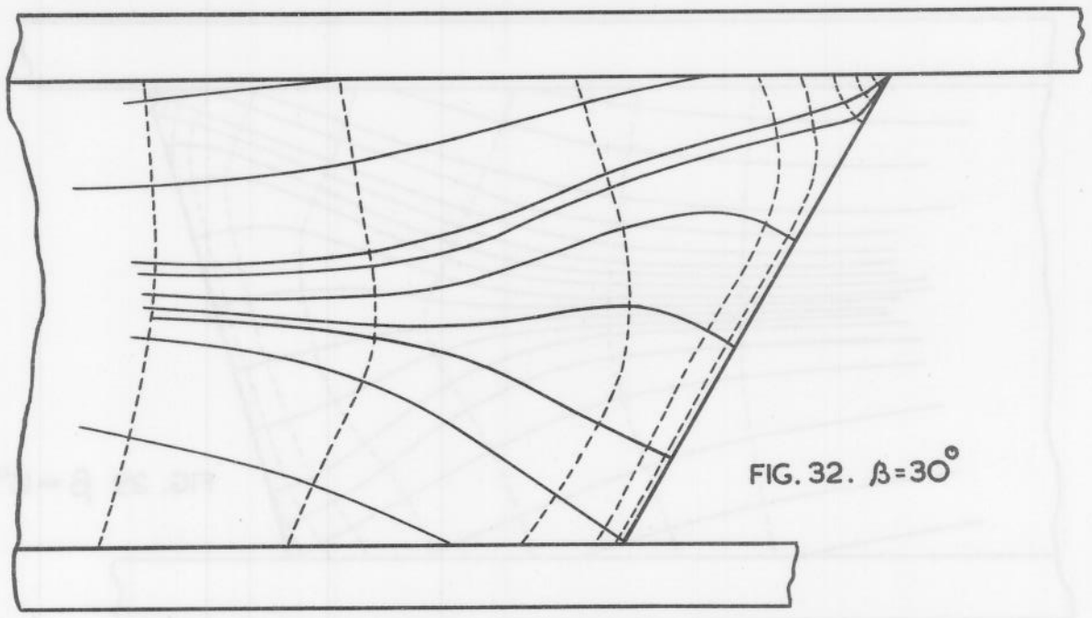

FIG. 32. $\beta = 30^{\circ}$

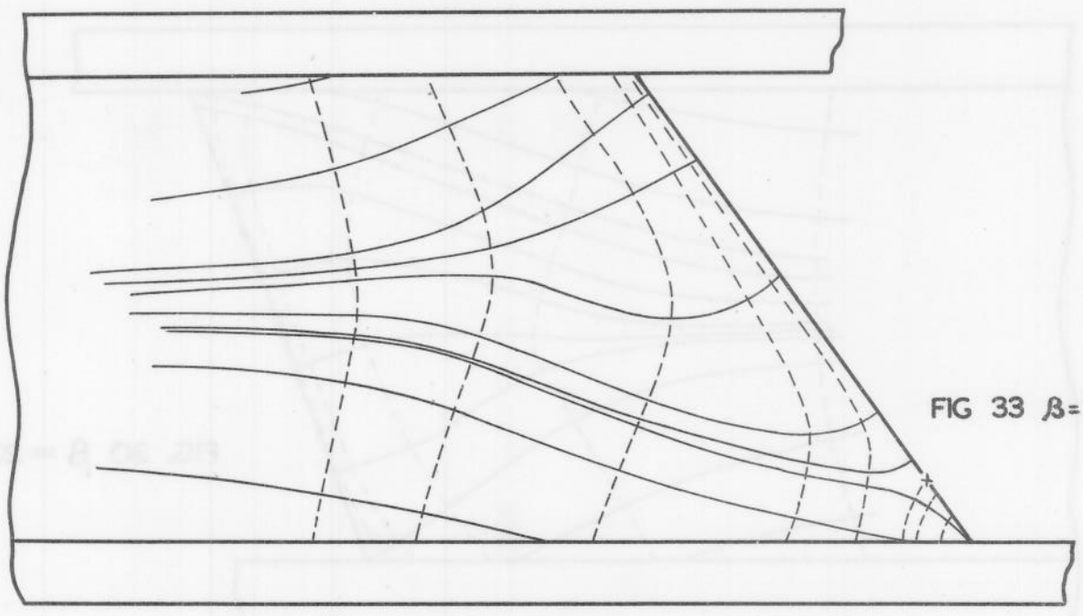

FIG 33 $\beta = 35^{\circ}$

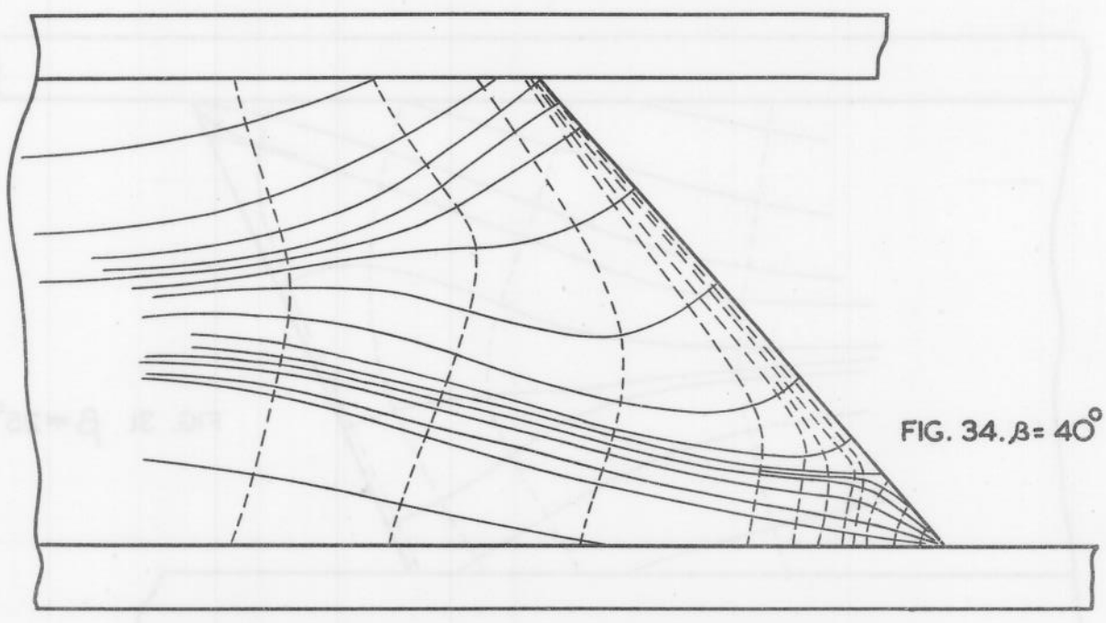

FIG. 34. $\beta = 40^{\circ}$

STRESS TRAJECTORIES

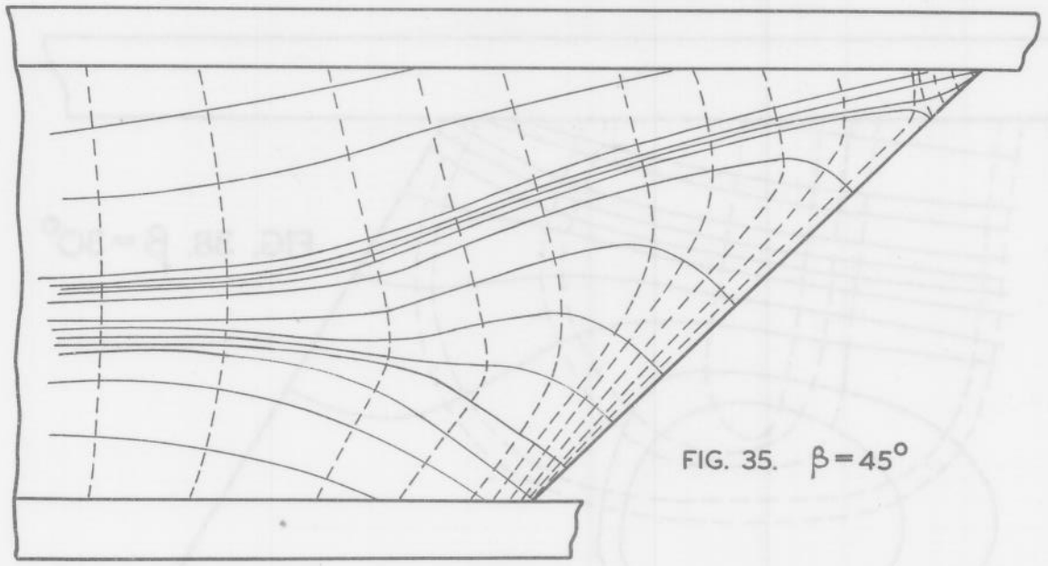

FIG. 35. $\beta = 45^\circ$

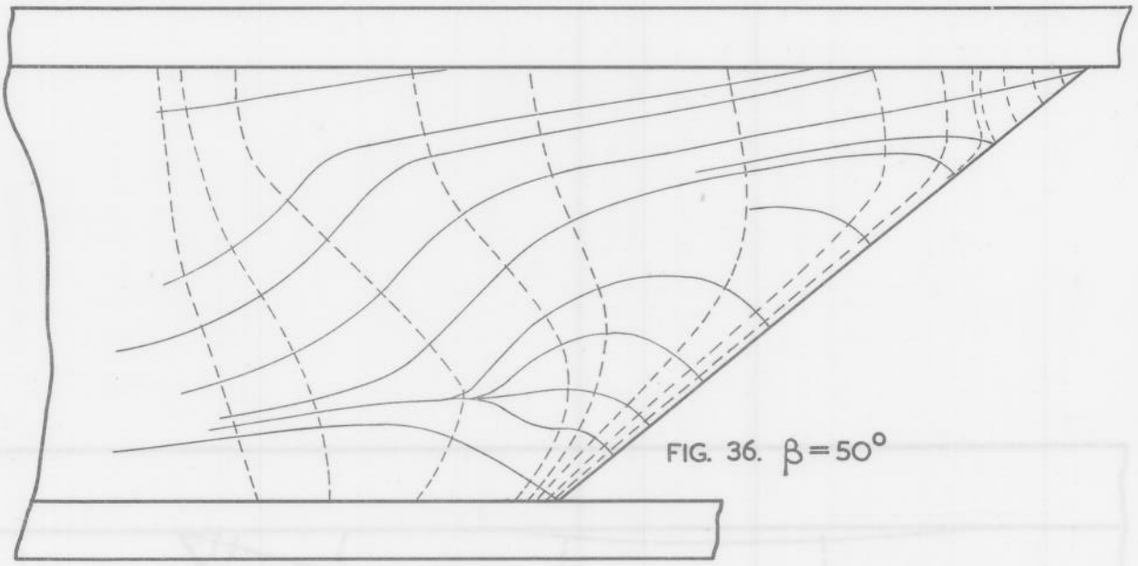

FIG. 36. $\beta = 50^\circ$

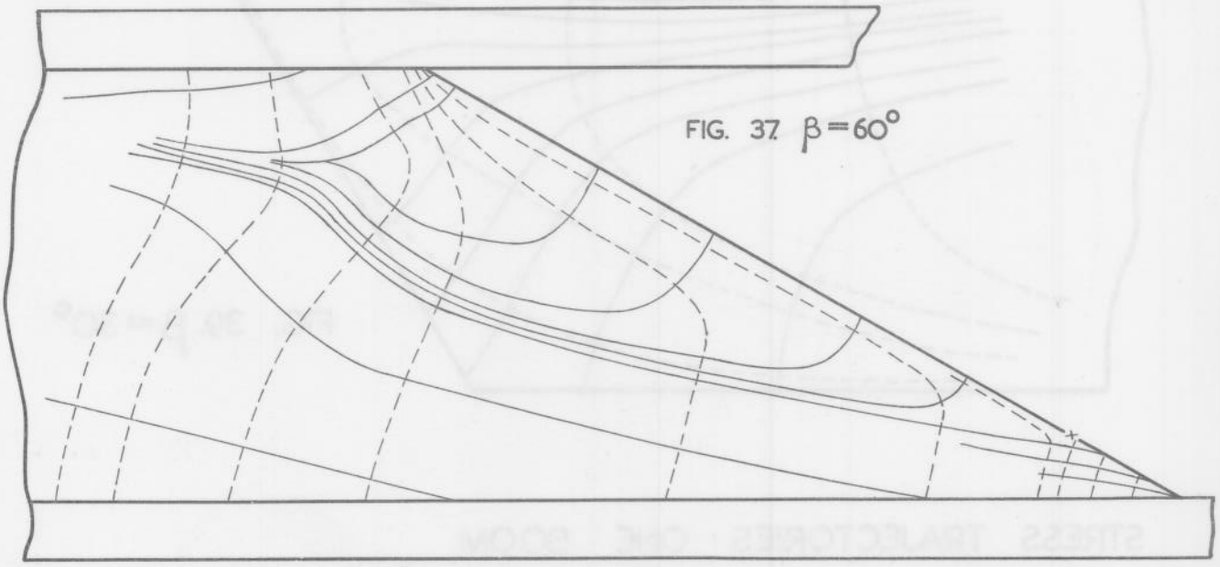

FIG. 37 $\beta = 60^\circ$

STRESS TRAJECTORIES

FIGS. 38 & 39.

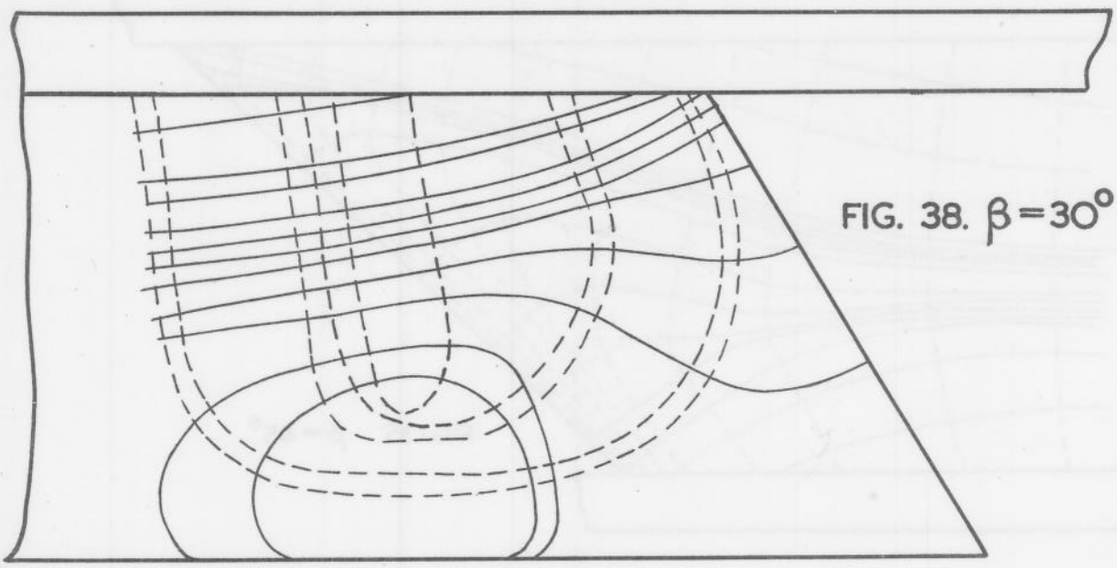

FIG. 38. $\beta = 30^{\circ}$

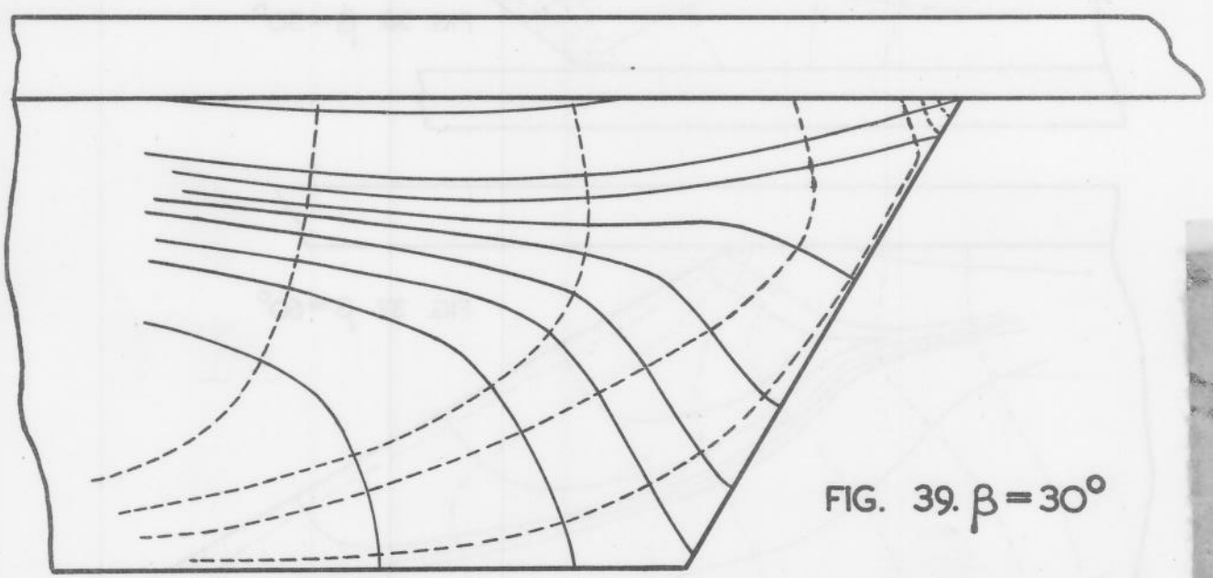

FIG. 39. $\beta = 30^{\circ}$

STRESS TRAJECTORIES ONE BOOM